To be presented at the International Solar Energy Society, American Section Annual Meeting, Denver, CO, August 28-31, 1978

A SOLAR TEST COLLECTOR FOR EVALUATION OF BOTH SELECTIVE AND NON-SELECTIVE ABSORBERS

Carl M. Lampert and Jack Washburn

August 1978

Prepared for the U. S. Department of Energy
under Contract W-7405-ENG-48

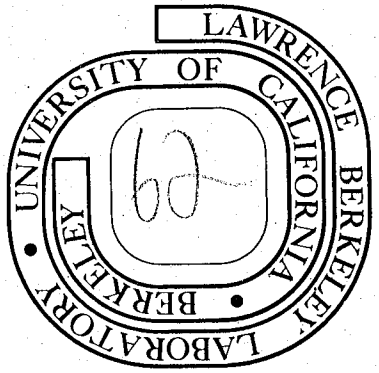

RECEIVED
LAWRENCE
BERKELEY LABORATORY
AUG 11 1978
LIBRARY AND
DOCUMENTS SECTION

A SOLAR TEST COLLECTOR FOR EVALUATION OF BOTH SELECTIVE AND NON-SELECTIVE ABSORBERS

Carl M. Lampert and Jack Washburn

Materials and Molecular Research Division,
Lawrence Berkeley Laboratory and
Department of Materials Science and Mineral Engineering,
College of Engineering; University of California
Berkeley, California 94720

ABSTRACT

A solar test collector was designed for the testing of thermally absorbing coatings under controlled conditions. The design consisted of a collector fed by a controlled temperature fluid within the range of 25-90°C (77-194°F). This temperature was maintained by a custom electronic controller. A small variable flow pump circulated water through three collector pipes at selected flow rates. Strip heaters coupled with a differential temperature controller compensated for edge losses associated with small collectors. Detailed design and operation data were presented and three black chrome and one non-selective absorber were analyzed in detail by test collector measurements. Results showed Efficiencies as high as 77% and 75% ($\Delta T = 0$) were obtained respectively for 1.0 μm black chrome on copper and nickel plated steel. The lowest loss coefficients were about 3.8 W/m^2°C for all black chrome/metal surfaces with the highest being 8.4 W/m^2°C for the black paint/metal sample.

1. EXPERIMENTAL APPARATUS AND PROCEDURES

A solar test collector was designed so that certain collector parameters could be held constant or controlled and yet different coatings could be tested. This design allows different types of selective and non-selective surfaces to be tested and evaluated in terms of collection efficiency under various operating temperatures and flow rates. Results for various Chromonyx coatings will be presented later and compared with those for a black painted surface.

In this study the collector was used to compare different types of black chrome (Chromonyx), supplied by Harshaw Chemical Co., and a black painted surface. These surfaces are representative of both selective and non-selective coatings and optical values of these coatings can be correlated to test collector data.

The main components of the collector consist of a body and cover, which houses three absorber pipes; a controlled temperature water bath; and a variable-flow pump.

The collector body is designed to permit easy removal of collector pipes. The body can be set any desired tilt angle with respect to the sun, to suit the season of the year. The collector pipes consist of a metallic material (e.g., copper or steel), although not a stringent requirement, coated with a selective or non-selective surface. Of the three parallel pipes, the center pipe is the critically controlled and monitored one. The purpose of the two outside pipes is to restrict the amount of heat lost from the sides of the central pipe. Furthermore, controlled temperature heating stripes are placed under the two outside pipes to reduce overall edge losses. In this fashion, a small collector can simulate large collector surroundings along the central pipe. This simulation is achieved by a differential temperature controller which maintains constant temperatures at all pipe outlets by turning on strip heaters when required. Across the central pipe both inlet and outlet temperatures are recorded with better than one degree (°C) accuracy.

The collector is fed by a controlled temperature bath which supplies a fluid at a set, adjustable temperature in the range 25-90°C. This temperature is maintained by a custom electronic controller. A small variable-flow pump circulates water through three collector pipes according to a specified but adjustable flow rate. The fluid from the collector is passed into a cooling bath and is recirculated to the controlled temperature water bath. Simultaneous measurements are made of solar radiation, ambient temperature, wind direction and velocity. The flow chart for the collector, showing the significant features described, is depicted in Fig. 1. A photograph of complete test apparatus is shown in Fig. 2. A detailed account of the total collector design is described elsewhere [1].

1.1. Controller System

The controller makes decisions and operates various heaters to compensate for outer collector pipe losses, and to regulate inlet water temperature.

The strip heater control system obtains its signals from the collector pipe outlet thermocouples. The outer pipe signals are compared to that of the central test pipe. Depending upon the difference

in signals the heaters will turn on or off independently.

Another circuit controls the water heater element. In this case the thermocouple signal is obtained at the inlet of the central pipe. This signal is compared to a set, adjustable voltage, calibrated in degrees. When the inlet temperature is lower than the set temperature, the water heater will operate. When the inlet temperature appears the same or greater (probably it will never greater than the set temperature) the heater will be off. The complete control diagram is depicted in Fig. 3. The accuracy of the controller is about $\pm 0.5^{o}C$ for each channel.

2. EXPERIMENTAL COLLECTOR RESULTS

The test collector results were obtained under clear sky conditions with wind velocity below 1.50 m/s from the northwest or west. Also, these results were obtained with solar radiation typically between approximately 600 to 1000 W/m^2 and with steady flow rates (for water) within the range of 2.45-49.2 L/hr. Typical inlet temperatures of 30, 35, 40, 45, 50 and $60^{o}C$ were used for the tests.

The types of surfaces tested were three selective absorbers of the Chromonyx black chrome type and one non-selective absorber of a commercial black spray paint. The non-selective absorber is made by Cal Custom/Hawk Company and it contains 4.8% black iron oxide in a modified silicone resin.

The designations and specifications of the absorbers are as follows:

R1 - 1.0 micron of black chrome on 12.7 microns of nickel on cold rolled mild steel.

R16 - 1.0 micron of black chrome on mild steel.

R9 - 1.0 micron of black chrome on copper.

HP1 - a thick coating (several hundred microns) of heat proof black paint on galvanized steel.

2.1 Calculation of Collector Efficiency

Another equivalent expression for instantaneous efficiency which is used for experimental data (a NBS proposed standard) is the following equation [2].

$$n = \frac{\left(\dot{m}\, C_p \int_{S_1}^{S_2} (T_{fe} - T_{fi})\, ds\right)/A_a}{\int_{S_1}^{S_2} I ds} \qquad (1)$$

where S_1 and S_2 represent limits of a time interval such as 0, 15-30 minutes;

A_a = the frontal area, receiving or aperture area (m^2);

C_p = the heat capacity of the fluid (J/kg ^{o}C);

$\dot{m}$ = the mass flow rate (kg/sec).

T_{fi} = inlet fluid temperature (^{o}C)
T_{fe} = exit fluid temperature (^{o}C)

I = solar radiation per unit time per unit area (w/m^2)

In Figures 4a-4d are shown the test collector results for the aforementioned samples. All lines are curve fit by a linear regression least squares approximation to represent the relationships of each of the curves; they are plotted in Fig. 5.

The equations, slopes and intercepts are shown in Table 1.

2.2 Calculation of Reflectance Parameters

By integration of $(1-r_w)$ where r_w is near-normal hemispherical spectral reflectance, over the solar spectrum the integrated absorptance (a_i) is obtained. Also, by integration of $(1-r_w)$ over the $100^{o}C$ blackbody spectrum the integrated emittance (e_i) is obtained. The higher the ratio of these values (a_i/e_i) the greater the selectivity.

The integrated results are shown in Table 2 for $20^{o}C$ measurements. From these results one can calculate the effective transmission absorption product $(ta)_e$ for the test collector. Also, the collector performance coefficient (F') and the loss coefficient (U_L) may be obtained [3]. These results are summarized in Table 3.

2.3 Discussion of Results

In some cases the scatter in the data points is representative of a situation one might expect for experimental conditions which would vary slightly with time. A true but very difficult procedure would be to control all collector parameters, except for insolation and resultant temperature differences, in such a way so they are time invariant. This might be achieved by the use of a completely simulated (fixed environment) collector.

An overall view of the data reveals that for the selective black chrome surface the data points for efficiency are mainly between 50-70%. These values indicate, under near optimal conditions, the efficiency at which the collector usually operates. The non-selective paint has 40-60% efficiency under the same conditions. The efficiency on the y-intercept is not a realistic operating point because the collector is at the ambient temperature ($\bar{T} = T_a$ or $\Delta T=0$). Frequently, this intercept value is mistakenly reported as optimum efficiency.

In reality, the curve fit for the data points is not linear except in the central region. Near the region of the y-intercept the curve should flatten out and in the region of the x-intercept the curve should dip downward. These effects occur because the loss coefficient (U_L) is a function of temperature. At higher temperatures the loss coefficient increases and at lower temperatures it decreases. The slope ratio between black paint and black chrome is approximately 2, which indicates that black paint will not perform as efficiently as black chrome at a given temperature. Also, the difference in x-axis intercept shows that black chrome will function at higher temperatures than black paint.

The black chrome plated copper pipe exhibits the highest net efficiency. This effect is due partially to the difference in thermal conductivity between copper and steel. Of the pipes tested, the copper pipe has approximately 2.5 the thermal conductance of the steel pipe. Choosing copper rather than steel for pipe material would depend upon the relative cost of materials and collector fluid flow rates (absorber heat transfer rate).

The effect of nickel plating steel creates only a slight rise in both the loss coefficient and efficiency of the absorber over that of black chrome directly on steel. (See Fig. 5).

3. CONCLUSIONS

A solar test collector has been designed and constructed which was used to measure the efficiency of four collector surfaces--three selective black chrome and one non-selective black paint. This collector was compensated for edge losses and measures differential pipe temperatures with 1°C accuracy. The absolute uncertainty of the collector measurements of efficiency are about 10% (for example a value of 60% efficiency could vary from 54-66%), while it has a few percent uncertainty in reproducibility and is limited by the accuracy of the mass flow rate measurement. The collector typically operates at low flow rates (0-49 L/hr) up to temperatures of 100°C at atmospheric pressure. The collector is designed so collector pipes may be removed with ease and it has the ability to regulate the fluid inlet temperatures within 1°C accuracy. The inlet temperatures are adjustable (25-90°C) and are maintained by an electronic controller. The collector includes a manual tilting stand for orientation to the sun.

The four surfaces tested (R1, R9, R16 and HP1) are representative of a range of possible combinations. The loss coefficients for these four surfaces show that black paint has about a factor of two times greater loss than for the black chrome samples. The loss coefficient for the black chrome samples was about the same--3.8 W/m^2 °C for all three. Black chrome on copper was the most efficient of the surfaces tested; probably, this is due to reflectance and high thermal conductivity of copper. Black chrome on nickel-plated steel and steel substrates had comparable properties. The effect of nickel plating steel accounted for only a 0.04 rise in efficiency for the absorber. Nickel plating may not be cost effective in light of this result. For the low flow rates at which the collector operated, the effect of the high thermal conductivity of copper is not a greater as it could be in promoting high heat transfer rates.

Spectral reflectance measurements are used to obtain optical parameters such as solar absorptance and infrared emittance. The best solar selectivity characteristics were exhibited by 1.0 micron of black chrome on copper (a_i/e_i = 18.5). Almost all combinations showed good selectivity. The effect of the nickel layer was marginal in promoting higher selectivity for the steel samples and it degraded selectivity on the copper samples.

4. ACKNOWLEDGMENTS

I am particularly grateful to Professor Jack Washburn for his guidance and support throughout this project. I wish to thank my colleague and friend, Dr. Lawrence Crooks, for his invaluable help help with the design and construction of the electronic controller. I am thankful to Mr. George Cunnington of Lockheed for his advice and use of spectral reflectance equipment.

This work was performed under the auspices of the U. S. Department of Energy.

5. REFERENCES

[1] C. M. Lampert, J. Washburn, LBL-6974, July 1978.

[2] NBS-National Bureau of Standards, U.S. Dept. of Commerce, Development of Proposed Standards for Testing Solar Collectors and Thermal Storage Devices, Technical Note, 899, 1976.

[3] J. A. Duffie and W. A. Beckman, Solar Energy Thermal Processes, Wiley, New York, 1974.

Table 1. Collection efficiency parameters of Figs. 4 and 5.

Type	Figure Number	Equation	Correlation Coefficient
R1	8a	= -3.6x + 0.75	r^2 = 0.992
R16	8b	= -3.3x + 0.71	r^2 = 0.973
R9	8c	= -3.5x + 0.77	r^2 = 0.979
HP1	8d	= -6.8x + 0.66	r^2 = 0.971

Type	Slope ($-F'U_L$) ($W/^oCm^2$)	y Intercept ($F'(ta)_e$)	x intercept ($^oCm^2/W$)
R1	-3.6	0.75	0.208
R16	-3.3	0.71	0.214
R9	-3.5	0.77	0.222
HP1	-6.8	0.66	0.097

Table 2. Integrated reflectance parameters.

	R1	R9	R16	HP1
a_i	0.958	0.942	0.92	0.95
e_i	0.070	0.051	0.070	0.832
a_i/e_i	13.7	18.5	13.1	1.14

Table 3. Collector performance and loss coefficients

	R1	R16	R9	HP1
$(ta)_e$	0.818	0.791	0.807	0.819
F'	0.916	0.898	0.954	0.806
U_L	3.9	3.8	3.7	8.4 ($W/^oCm^2$)

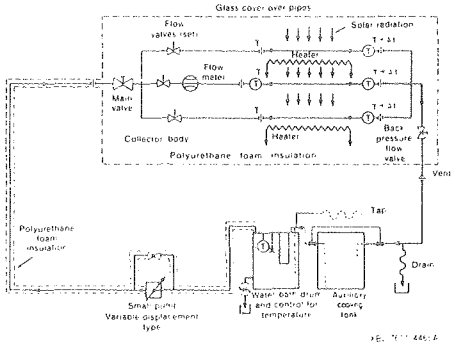

Fig. 1. Solar test collector flow chart.

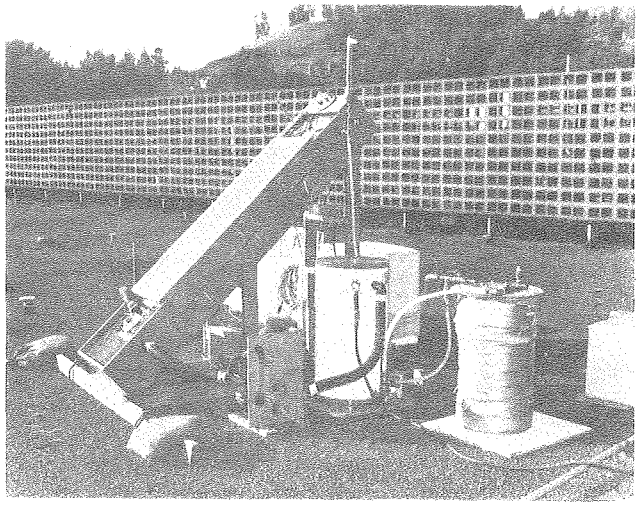

Fig. 2. Solar test collector in operation, side view. CBB 770-9662

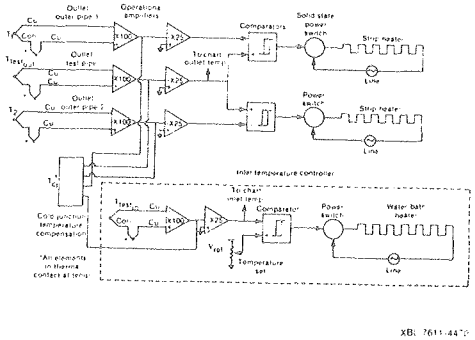

Fig. 3. Electronic control design showing how string heaters and waterbath temperature are controlled automatically.

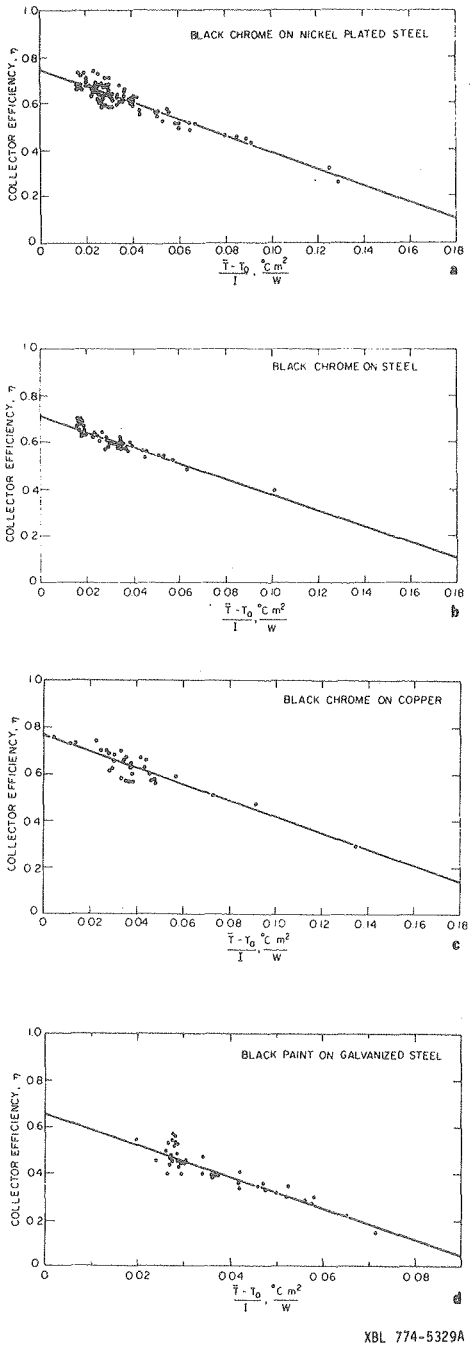

Fig. 4. Efficiency versus ratio of average temperature above ambient and solar radiation.

a) Black chrome on nickel plated steel (R1).

b) Black chrome on Steel (R16).

c) Black chrome on Copper (R9).

d) Black paint on galvanized steel (BP1).

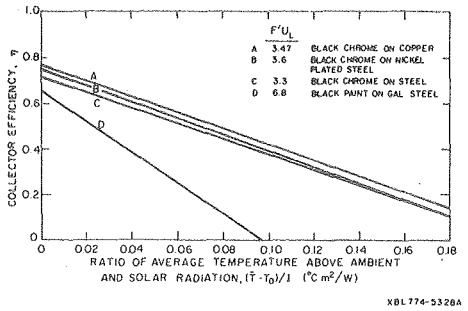

Fig. 5. Comparative efficiency plots for absorber surfaces in Fig. 4. F' and U_L are respectively the collector performance and loss coefficients.

This report was done with support from the United States Energy Research and Development Administration. Any conclusions or opinions expressed in this report represent solely those of the author(s) and not necessarily those of The Regents of the University of California, the Lawrence Berkeley Laboratory or the United States Energy Research and Development Administration.